Analytical Approximation Techniques in Background Loop Quantum Cosmology

MR4180

MSc Dissertation in

Masters in Research in Physics

2015/16

School of Physics and Astronomy

University of Nottigham

Anshuman Bhardwaj

Supervisor: Professor Edmund J.Copeland

I have read and understood the School and University guidelines on plagiarism. I confirm that this work is my own, apart from the acknowledged references.

Abstract

In this report we present analytical approximation techniques to describe how a scalar field with an arbitrary potential evolves in the background of a quantum FLRW spacetime described by LQC. In general there is an initial phase of superinflation independent of the shape of the potential, then there is a damping phase which leads to turnaround and then finally we have a phase of slow-roll inflation. The percentage error between the values of observables (like scalar field ϕ and its derivative $\dot{\phi}$) predicted by the analytic and numerical data are in general less than 5 percent and this is shown in tables. These analytical techniques work very well for all cases of the potentials (quadratic, Starobinsky and quartic) we have considered here except for the potential energy dominated regime of the Starobinsky potential. The reason is that due to the nature of the regime there we have to use damping equations several times to reach the bottom of the potential where the next regime starts which makes it infeasible. Thus we propose an alternate way of analytically understanding that regime which agrees with the numerical results.

Contents

List of Figures

1 Introduction

The 20th Century saw the rise two great theories : General Relativity(GR) and Quantum Mechanics(QM). General Relativity could explain not just Newton's laws but also the large scale structure of spacetime. It predicted the existence of black holes and that our universe came from an accelerating era in the past, known as inflation. But it fails at the centre of the black hole and at the big bang instant which is the famous singularity problem of GR. On the other hand QM was able to explain the microscopic world i.e. the atoms, molecules, nucleus and all of its particle contents like the quarks and leptons. But it possesses infinities which can be overcome by a procedure known as renormalization. Thus both of these theories are successful in describing the large(GR) and the small(QM). But what about objects or processes that are large/massive but can still be squeezed(or certain parts of them) to an extremely small size, i.e. what happens close to a singularity or what happens to entanglement near a black hole horizon? These questions beg for a theory of Quantum Gravity which we don't have right now as it is extremely difficult to combine GR and QM. To date we have a collection of different approaches each of which have their own strengths and weaknesses : String Theory [1,2], Loop Quantum Gravity [3-6], Causal Dynamical Triangulation[7], Causal Sets[8] and others.

In this dissertation we will touch on one of those approaches : Loop Quantum Gravity(LQG), specifically its application to cosmology : Loop Quantum Cosmology(LQC). It is a framework which tries to combine Quantum Mechanics and General Relativity by first writing GR in a Hamiltonian form in the Holonomy and Triad variables which when quantized become operators which act on states which represent quantum geometry. The result is the existence of an area operator whose smallest eigenvalue represents the minimum area spacetime can have. The kinematic side is under control but the dynamics is under development which leads to the problem that currently LQG doesn't reproduce GR as its semicalssical limit.

LQC [9-13] is a quantum reduced model of LQG where one ignores all spatially inho-

mogeneous degrees of freedom in the metric and retains only the scale factor, a, and its conjugate momenta $\dot{a} \equiv da/dt$ and then quantizes it. This means that the wavefunction of the universe which could have had a spread in all possible degrees of freedom in the metric $g_{\mu\nu}$ is now restricted to spread only in two degrees of freedom $(a, \dot{a})$. It is a minisuperspace model which violates the uncertainty principle and this is one of key problems because one can ask whether its implementation in cosmology can be trusted or not. However one could also compare this with Dirac theory of Hydrogen atom. Here we consider a proton-electron system where we use spherical symmetry to reduce the Maxwell theory and then quantize which curbs many degrees of freedom too but still gets much deeper structure like spin (except for the Lamb shift) than just applying the Schrodinger's equation to Hydrogen atom. However Quantum Electrodynamics was developed bringing with it the associated power of Feynmann diagrams along with the corresponding creation and annihilation operators of electron and positron pairs which could explain the Lamb shift. So hopefully when the full LQG will be developed, then the corrections over LQC results may be very small[14]. Steps are being taken in this direction[15,16].

In a nutshell LQC is constructed by first writing GR(reduced to cosmological degrees of freedom) and then using LQG techniques to construct the Kinematical Hilbert Space of quantum geometry states for FLRW spacetime. This gives a quantum Hamiltonian constraint which can be used to study the evolution of scale factor of universe. This leads to a resolution of the Big Bang singularity by replacing it with a Big Bounce. This is achieved in two ways: firstly the solutions go right through the $t = 0$ point in time. Secondly, for sharply peaked states the quantum Hamiltonian constraint reduces to a an effective Friedmann equation which approximates the underlying quantum theory very well (Figure 1). This effective Friedmann equation makes the Hubble parameter go to zero at the point where the matter density reaches its maximum(almost half of the Planck density)[9-13]. Also LQC has a well defined classical limit in which for matter densities much less than the Planck density we recover the effective Friedmann equations. Perturbations have also been studied deeply[17-19]. A mathematical framework has been

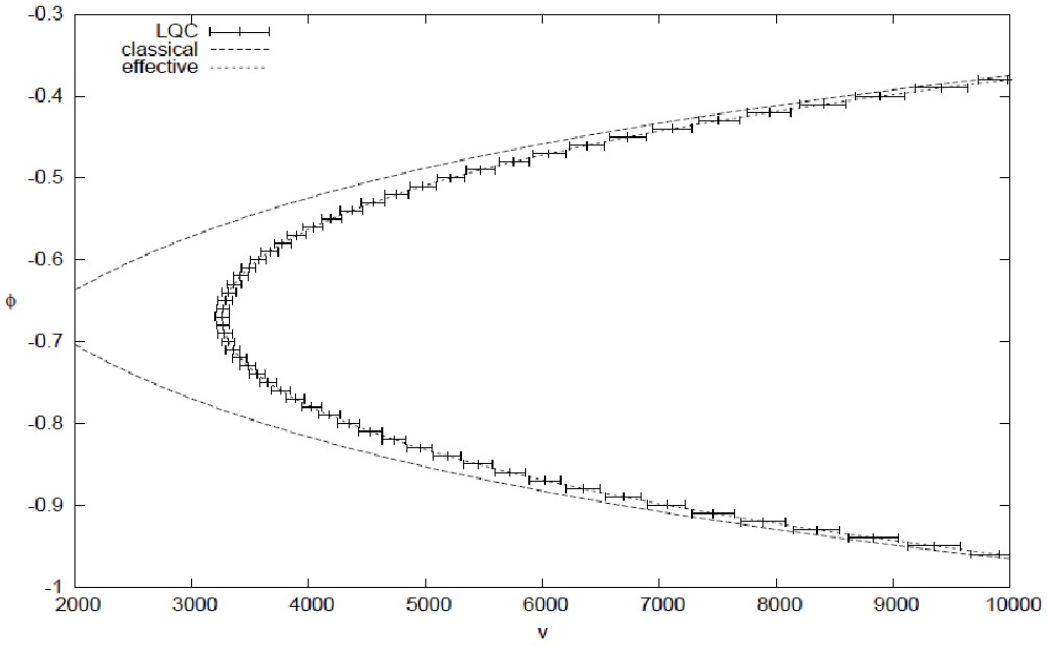

Figure 1: Expectation values and dispersions of volume of the universe $v = a^3$(where a is the scale factor) obtained from the LQC Hamiltonian constraint are plotted against the scalar field ϕ(which serves as time here) and compared with the results obtained from the effective Friedman equation and classical GR. This shows that the effective dynamics provides a good approximation to the underlying quantum theory. Unlike GR where the volume of the universe drops to zero at the Big Bang, in LQC the universe starts with a contracting phase, reaches a minimum volume at the Big Bounce and enters into an expanding phase. Taken from [11].

developed to deal with quantum fields(like the scalar field perturbations) propagating on quantum FLRW spacetime[17] which assumes that the perturbations are like test fields and thus there is no quantum backreaction. The result is that propagation of quantum fields on quantum FLRW spacetimes is exactly the same as propagation of quantum fields on classical FLRW spacetime which is dressed/modified with quantum corrections coming in it in terms of $\hbar$. This has been used in the numerical study of the evolution of scalar fields and their perturbations on a LQC background with both quadratic [20,21] and Starobinsky [22,23] scalar field potentials. This has been done both at the levels of background and perturbations. The results show that for most of the initial conditions the results match with standard inflation and only for small set of initial conditions there are significant deviations(large angular scale power suppression) which can help us to phenomenologically explain the CMB anomalies and thus have contact with future experiments[18,19]. So the area has matured enough to start making contact with observations and this is a great achievement.

For this dissertation we just need to understand the background evolution of the inflaton field on the LQC spacetime. Let us discuss one example which is based on numerics. We have a potential say quadratic[20,21] where the values of the field are bounded because the maximum energy density at the bounce is fixed. This automatically fixes the range of initial conditions for the inflaton. Suppose we start at the bottom of the potential then the Kinetic energy at the bounce will be dominating. Thus the inflaton will roll up the potential until it reaches a regime where the potential energy becomes important and causes the inflaton to momentarily stop and then turn around. Soon the standard slow-roll starts and finally the inflaton reaches the bottom most point and stops. In this paper we will describe this whole behaviour by breaking up this entire journey into several phases each of which has its own approximation which simplifies the task of obtaining the solutions. Thus our results are analytic and do not depend on the numerics. This analytic approach describes why the scalar field behaves the way it does.

The plan of this dissertation is as follows. In Section 2 we will discuss what are the

basic equations which govern the evolution of a scalar field on an effective semiclassical spacetime described by LQC. We will determine the various possible cases that can arise due to different initial conditions at the bounce. We will also define the various inflationary observables and how to find their values at the pivot point. In Section 3 we will discuss how to divide the whole journey of the scalar field on any potential into different phases in particular an initial phase of Kinetic Energy(KE) domination, then a Potential Energy(PE) dominating phase and finally the Slow-roll phase. This division differs for Kinetic and Potential dominating cases at the bounce. For each of the phases we will obtain analytical expressions for the inflaton observables $(\phi, \dot{\phi})$. In Section 4 we will describe how we get the analytic data and compare it with numerics and show that they match on to each other to within a few percent. In Section 5, we will summarise our results and discuss future possibilities.

The notations we will be using in this dissertation are as follows (unless stated otherwise): We will work in the units $\hbar = c = G = 1$ i.e. the Planck units $m_{Pl} = l_{Pl} = t_{Pl} = 1$ and we will assume that there is no cosmological constant and that the universe is spatially flat i.e. $\Lambda = 0 = k$.

2 The Framework

The two basic equations that we are going to use are : The effective Friedman equation with holonomy corrections[9,11-13,18-24] and the Continuity equation. These describe the evolution of scalar field on the LQC spacetime with arbitrary potential.

$$H^2 = \frac{8\pi}{3}\rho\Big(1 - \frac{\rho}{\rho_c}\Big) \tag{2.1}$$

$$\ddot{\phi} + 3H\dot{\phi} + V'(\phi) = 0 \tag{2.2}$$

where $\rho = \frac{\dot{\phi}^2}{2} + V(\phi)$, $V'(\phi) = dV/d\phi$ and $H = \frac{1}{a}\frac{da}{dt}$ is the Hubble parameter where $a(t)$ is the scale factor. The critical density is given by $\rho_c = \frac{\sqrt{3}}{32\pi^2\gamma^3} m_{Pl}^4 \approx 0.41$ where

$\gamma = 0.2375$ is the Barbero-Immirzi parameter. There is no general analytic expressions for the observables $(a, \dot{a}, \phi, \dot{\phi})$ which satisfies (2.1) and (2.2) as this combination gives a complex non-linear differential equation. These equations have been studied numerically for quadratic potential, $V(\phi) = \frac{1}{2}m^2\phi^2$, in [20,21] and Starobinsky potential, $V(\phi) = \frac{3M^2}{32\pi G}\left(1 - e^{\sqrt{16\pi G/3}}\right)^2$, in [22,23]. Let us understand some general aspects about the evolution of such a system of equations. The picture here is very simple : Take any potential $V(\phi)$. It cannot take arbitrary values as the total energy density satisfies the constraint :

$$0 \leq \rho \leq \rho_c \tag{2.3}$$

which is because of the properties of Big Bounce coming from (1) (i.e. $H = 0$ at $\rho = \rho_c$ and it is symmetric around this density, thus the universe has a contracting branch in the past, reaches a minimum volume and then expands again). When we start at the bounce $\rho = \rho_c$ then $\frac{\dot{\phi}^2}{2} + V(\phi) = 0.41$. Thus the values that $\dot{\phi}$ and ϕ(and also $V(\phi)$) will be bounded at the bounce(exception: for the Starobinsky case, ϕ can have very large values at the bounce for $\phi \gg 0$ side of the potential). This decides whether the initial conditions are Kinetic Energy(KE) or Potential Energy(PE) dominated. The inflaton can start by sliding up ($\dot{\phi}_B > 0$) or sliding down ($\dot{\phi}_B < 0$). In any case the total energy ρ will decrease with time because of the friction term in (2). Note that a subscript 'B' denotes bounce and QG denotes quantum gravity.

Kinetic Energy domination at the Bounce, i.e. $KE_B \gg PE_B$. Suppose the inflaton starts at the bottom of a quadratic potential and with a positive velocity $\dot{\phi}_B > 0$. It will first experience a regime where Kinetic Energy is dominating which we will call as QG assisted Kinetic Regime because of the holonomy correction in (2.1). This regime includes a phase of superinflation where the Hubble parameter rapidly increases to its maximum value $\sqrt{\frac{2\pi\rho_c}{3}}$ at half of the critical density. It is an extremely short lived phase. Then comes a regime where the KE and PE are comparable and this includes the equilibrium point where $KE = PE$. Then comes a PE dominated regime which we will call as Damp-

ing regime. It is not QG-assisted as the density here has dropped to $\rho \sim 10^{-11}\rho_{Pl}$. In this regime the inflaton slows down and reaches the turnaround point($\dot{\phi} = 0$) and then rolls down to a point where $\ddot{\phi} \approx 0$ which marks the beginning of the Slow-roll regime. In this the inflaton will pass through the pivot $\phi = \phi_\star$ (which corresponds to the largest CMB mode observable today and so connects theory with observations). Then some initial conditions are excluded and others kept depending on whether they lead to desired slow-roll. If suppose the inflaton had started somewhere slightly up the potential but still kinetic dominated at bounce and with negative velocity, then there would again be a QG-assisted Kinetic regime, then a damping regime with no turnaround and finally a slow-roll point. Again the inflaton must reach the pivot point with the right conditions so that desired slow-roll is achieved.

Potential Energy domination at the Bounce. The inflaton starts in a damping regime but still following (2.1) with QG-corrections and thus we will call this QG-assisted Damping Regime as now we are high enough in the potential to have $\rho \sim \rho_c$. Depending on whether the inflaton starts with positive or negative velocity, there may or may not be a turnaround point. But there can be a slow-roll regime which may or may not be the desired one depending on the conditions at the pivot point.

During this evolution one would like to know how the various observables like the scale factor, the Hubble parameter, scalar field and their derivatives. In general this is done numerically as the equations are hard to handle. But in the next section we will be getting explicit expressions for $(\phi, \dot{\phi})$ in different approximation regimes. So we will be able to calculate the above list of observables analytically. It will be good at this point to discuss what we exactly mean by this. Suppose in a certain regime we are allowed to use a set of approximations on (2.1)-(2.2). If the resulting differential equations are simple enough, then they can be solved analytically to obtain the expression for $\phi(t)$. We can differentiate this to get the expression for $\dot{\phi}$. We will treat $(\phi, \dot{\phi})$ as our PRIMARY

observables. They will serve as the building blocks for the above mentioned observables like $\ddot{\phi}, H, \dot{H}, \epsilon_H ...$ etc which we will call as SECONDARY observables. It is important to note that we have put $\ddot{\phi}$ in the category of secondary observables. We will define this when we come to equation (2.9) and discuss in Section 4. First let us individually look at the general formulas for the observables : $(\dot{H}, \epsilon_H, \epsilon_V, \eta_H, \eta_V, w, N)$

- Differentiate (1) to get :

$$\begin{aligned} \dot{H} &= \frac{8\pi}{6}\frac{\dot{\rho}}{H}\Big(1-\frac{2\rho}{\rho_c}\Big) \\ &= -4\pi(\rho+p)\Big(1-\frac{2\rho}{\rho_c}\Big) \\ &= -4\pi\dot{\phi}^2\Big(1-\frac{2\rho}{\rho_c}\Big) \end{aligned} \tag{2.4}$$

where in the second line we have used the alternative form of (2) i.e. $\dot{\rho} = -3H(\rho+p)$ and in the third line we have used $\rho = \frac{\dot{\phi}^2}{2} + V(\phi)$ and $p = \frac{\dot{\phi}^2}{2} - V(\phi)$. Note that the only source of energy density is the scalar field, ie we are ignoring any matter or radiation.

- The slow-roll parameters :

$$\begin{aligned} \epsilon_H &= -\frac{\dot{H}}{H^2} \\ &= \frac{3\dot{\phi}^2(\rho_c - 2\rho)}{2\rho(\rho_c-\rho)} \qquad (2.5) \\ &= \frac{3(\rho_c-2\rho)(\rho-V)}{\rho(\rho_c-\rho)} \qquad (2.6) \end{aligned}$$

where in the second line we have used (1) and (4). In the slow-roll regime this is equal to $\epsilon_V = \frac{1}{16\pi}\Big(\frac{V'}{V}\Big)^2$. Similarly we have η_H and η_V.

- Then we have the equation of state and the number of e-folds :

$$w = \frac{KE-PE}{KE+PE} = \frac{\dot{\phi}^2 - 2V(\phi)}{\dot{\phi}^2 + 2V(\phi)} \tag{2.7}$$

$$N = \log\frac{a(t_f)}{a(t_i)} = \int_{t_i}^{t_f} H dt \tag{2.8}$$

where we integrate from an initial time t_i to a final time t_f.

- Finally we will define a new observable:

$$\ddot{\phi} = -3H\dot{\phi} - V'(\phi) \tag{2.9}$$

We have defined it using the continuity equation (2.2). Numerically there is no difference in the two possible definitions of $\ddot{\phi}$ i.e $\ddot{\phi} = \frac{d\dot{\phi}}{dt}$ and $\ddot{\phi} = -3H\dot{\phi} - V'(\phi)$. But as we will see later the second definition is more useful for our analytic discussion.

Before we conclude this section we would like to talk about the 'pivot-point' which connects theory with observations. Whether we do numerics or analytics we need the value of the mass parameter in the inflaton potential. We first ask what is the largest observable mode of CMB? The answer is $k_* = 0.002 Mpc^{-1}$ and this gives the value of the amplitude of scalar perturbations A_s and spectral index n_s. The time t_* at which the mode k_* exited the horizon, at that time we need to determine 6 unknowns $(\epsilon, \eta, H, \phi, \dot{\phi}, M)$. For this we require the values of n_s, A_s, the number of e-folds from the time when k_* exited the horizon to the end of slow-roll inflation defined by $\epsilon = 1$ and 6 equations :

$$A_s = \frac{H_*^2}{\pi \epsilon_*} \tag{2.10}$$

$$n_s - 1 = -4\epsilon_* + 2\eta_* \tag{2.11}$$

$$N_* = -8\pi \int_{\phi_*}^{\phi_{end}} \frac{V(\phi)}{V'(\phi)} d\phi \tag{2.12}$$

$$3H_*\dot{\phi}_* + V'(\phi_*) \approx 0 \tag{2.13}$$

$$H_*^2 = \frac{8\pi}{3}\left(\frac{\dot{\phi}_*^2}{\dot{\phi}_*^2 + 2V(\phi_*)}\right) \tag{2.14}$$

$$\epsilon_* = \frac{3\dot{\phi}_*^2}{\dot{\phi}_*^2 + 2V(\phi_*)} \tag{2.15}$$

So if one knows the values of n_s, A_s and N, all the unknowns at the pivot-point can be evaluated, the most useful of which is ϕ_* and the mass parameter in the potential.

For the quadratic potential we can use equations (2.10)-(2.15) to find $\phi_* = \pm 3.15$ and $m = 1.21 \times 10^{-6}$ as is done in [21].

3 The Different Phases of Evolution

As promised we will now break the evolution of the inflaton field rolling on the potential-hill into different regimes in two different ways depending on whether the bounce is KE or PE dominated. We will study each of these regimes in detail and discuss what approximations can be used to derive analytic expressions for the observables.

3.1 Kinetic Energy Domination at the Bounce

This corresponds to the case where $\frac{PE_B}{\rho_c} < \frac{1}{2}$.

3.1.1 QG-assisted Kinetic/Superinflation Regime

In this regime, Kinetic energy(KE) dominates over the Potential Energy(PE). We will introduce two approximations here : Firstly, we have $\frac{\dot{\phi}^2}{2} \gg V(\phi)$ thus the total energy $\rho \approx \frac{\dot{\phi}^2}{2}$ and secondly, we will assume $\ddot{\phi} \gg V'(\phi)$. Thus the basic equations (1) and (2) in this regime become :

$$H^2 = \frac{8\pi}{3}\rho\big(1 - \frac{\rho}{\rho_c}\big) \tag{3.1}$$

$$\ddot{\phi} + 3H\dot{\phi} = 0 \tag{3.2}$$

$$\rho = \dot{\phi}^2/2 \tag{3.3}$$

We can solve these equations following [24]. Setting the initial condition as $(\phi, \dot{\phi}) = (\phi_B, \sqrt{2\rho_c})$ at $t = 0$, we get the following expressions:

$$\dot{\phi}(t) = \frac{\sqrt{2\rho_c}}{\sqrt{1 + 24\pi\rho_c t^2}} \tag{3.4}$$

$$\phi(t) = \phi_B + \frac{1}{\sqrt{12\pi}} \sinh^{-1}(\sqrt{24\pi\rho_c}t) \tag{3.5}$$

We will call equations (3.4)-(3.6) superinflation solutions as superinflation occurs in this regime. Superinflation is a period where the Hubble parameter rapidly increases from zero at the bounce to a maximum value of $\sqrt{2\pi\rho_c/3}$. This is achieved after a time $t = (24\pi\rho_c)^{-1/2} \approx 0.18$ Planck seconds. In this period the scale factor increases independent of any potential as:

$$a(t) = (1 + 24\pi\rho_c t^2)^{1/6} \tag{3.6}$$

Notice that expressions (3.4)-(3.5) are general in nature and don't depend on $V(\phi)$. This is because we have assumed from the beginning that in this KE-dominated regime the potential and its derivatives do not play any significant role in the equations. However this may not hold for all potentials. For example take the case of monodromy potential $\phi^{2/3}$ which has $V'(\phi) \propto \phi^{-1/3}$. This becomes unbounded near the origin.

So how long does this KE dominated regime last, i.e. at what point of time do we end this regime? To a first approximation we can say it lasts until the KE and PE are equal, a point we call the equilibrium point. We have the expressions for $\phi(t)$ and $\dot{\phi}(t)$ from equations (3.5) and (3.6).The equilibrium point therefore satisfies the condition

$$\frac{\rho_c}{1 + 24\pi\rho_c t^2} = V\Big[\phi_B + \frac{1}{\sqrt{12\pi}} \sinh^{-1}(\sqrt{24\pi\rho_c}t)\Big] \tag{3.7}$$

This is an equation in t which we can solve numerically to get the time taken to reach the equilibrium point t_{eq}. After we get t, we plug it back into the expressions (3.5)-(3.6) to get $(\phi_{eq}, \dot{\phi}_{eq})$. How do these analytic solutions compare with numerics? For the case of the quadratic potential from Table 1 with $\phi_B = 1.06$, at the Equilibrium point, the value of $(\phi, \dot{\phi})$ predicted by (3.5)-(3.6) is $(3.19, 3.86 \times 10^{-6})$ as opposed to the values obtained using the full numerical solutions [21], $(3.16, 3.82 \times 10^{-6})$ with percentage errors as $(0.95, 1.05)$. The other observables also behave in the same way. Thus we can be confident that our analytics mimic the numerics to excellent accuracy and we can trust them for further discussions.

It may seem strange that we have used the idea of ignoring the PE (compared to KE) and $V'(\phi)$ (compared to $\ddot{\phi}$) to derive (3.4)-(3.6) and then we are using these solutions to describe the behaviour even up till the equilibrium point where PE is no longer ignorable and yet, the analytics seem to work very well. Why is that? To answer this let us look at averages defined as :

$$< A >= \frac{\int_0^{t_{eq}} A(t)dt}{\int_0^{t_{eq}} dt} \tag{3.8}$$

Using this we would like to see how $\frac{<V'(\phi)>}{<\ddot{\phi}>}$ and $\frac{<V(\phi)>}{<\dot{\phi}^2/2>}$ behave from the bounce to the equilibrium point. We can do that either analytically i.e use equations (3.5)-(3.6) to find the averages or we can simply use the numerical solutions. Both of them agree with the general behaviour of these averages. First let us consider $\frac{<V(\phi)>}{<\dot{\phi}^2/2>}$. Its value is of order $10^{-6} - 10^{-7}$ for all the potentials in this (KE dominated) regime. Thus it justifies our approximation for ignoring the PE with respect to KE in (3.1)-(3.3). One may ask why not consider averages like $\left\langle \frac{V}{K} \right\rangle$ or $\left\langle \frac{K}{V} \right\rangle^{-1}$ where $K = \dot{\phi}^2/2$. The reason is that for all potentials $\left\langle \frac{K}{V} \right\rangle^{-1} \approx 10^{-7}$ which again justifies our approximation but $\left\langle \frac{V}{K} \right\rangle \approx 0.3$ which means the PE contributes about a quarter of the total energy density on average. Thus this average does not justify our approximations so well, even though the numerics and analytics agree upon the value of $\left\langle \frac{V}{K} \right\rangle \approx 0.3$ itself! Now the ratio $\ddot{\phi} : 3H\dot{\phi} : V'$ is $1 : 1 : 10^{-7}$ for quadratic/quartic and $1 : 1 : 10^{-9}$ for Starobinsky potential. This justifies the approximation that $V'(\phi)$-term can be ignored with respect to the other terms in the Continuity equation.

The end of this regime gives us $(\phi_{eq}, \dot{\phi}_{eq})$ at the equilibrium point which serve as the initial conditions for the next phase.

3.1.2 The Damping Regime

Just as in the previous regime, here also we will make two primary approximations : Firstly, the total energy density is much less than the critical density($\rho \ll \rho_c$). Secondly, we will ignore the KE with respect to PE i.e. $V(\phi) \gg \frac{\dot{\phi}^2}{2}$ which gives $\rho \approx V(\phi)$ but this time retaining both $\ddot{\phi}$ and $V'(\phi)$ in the continuity equation. Thus the basic equations (1)

and (2) here become :

$$H^2 \approx \frac{8\pi}{3}\rho \tag{3.9}$$

$$\ddot{\phi} + 3H\dot{\phi} + V'(\phi) = 0 \tag{3.10}$$

$$\rho \approx V(\phi) \tag{3.11}$$

Combining them gives us :

$$\ddot{\phi} + \sqrt{24\pi V(\phi)}\dot{\phi} + V'(\phi) = 0 \tag{3.12}$$

Now we will introduce a secondary approximation. Since this is a potential energy dominated regime therefore the inflaton moves very slowly such that $\dot{\phi} \approx 0$. Thus changes in ϕ say from the equilibrium till turnaround/slow-roll point are very small. This can be seen from Table I for the quadratic potential for the case $\phi_B = 1.06$, $(\phi_{Turn} - \phi_{eq}) = 0.13$ while $(\phi_{eq} - \phi_B) = 2.13$. Thus we will Taylor expand all the functions of ϕ around ϕ_{eq} to linear order keeping in mind the errors.

Equation (3.12) looks very similar to a damped harmonic oscillator. Taylor expanding the potential and its derivatives (exception: monodromy) around the equilibrium point, we obtain :

$$\begin{aligned} V(\phi) &= V(\phi_{eq}) + (\phi - \phi_{eq})V'(\phi_{eq}) + O(\phi - \phi_{eq})^2 \\ V'(\phi) &= V'(\phi_{eq}) + (\phi - \phi_{eq})V''(\phi_{eq}) + O(\phi - \phi_{eq})^2 \end{aligned} \tag{3.13}$$

Numerically we can evaluate these expressions at the Turnaround point (as this is the farthest the inflaton goes away from the equilibrium point) and ask what percentage do the linear order corrections in $V(\phi)$ and $V'(\phi)$ occupy i.e. calculate $\frac{(\phi_{Turn}-\phi_{eq})V'(\phi_{eq})}{V(\phi_{Turn})} \times 100$ and $\frac{(\phi_{Turn}-\phi_{eq})V''(\phi_{eq})}{V'(\phi_{Turn})} \times 100$ respectively. For quadratic potential we get these to be 8 percent and 4 percent respectively. For Starobinsky potential we get these to be 2 percent and 35 percent respectively. This shows that we can ignore the corrections in $V(\phi)$ in general but we cannot ignore the corrections in $V'(\phi)$. Also we will define a new variable

$\psi = \phi + \frac{c}{b}$, where $b = V''(\phi_{eq})$ and $c = V'(\phi_{eq}) - \phi_{eq}V''(\phi_{eq})$. Thus $\dot{\psi} = \dot{\phi}$ and $\ddot{\psi} = \ddot{\phi}$ and the evolution equation for this regime becomes :

$$\ddot{\psi} + a\dot{\psi} + b\psi = 0 \tag{3.14}$$

where $a = \sqrt{24\pi V(\phi_{eq})}$ and $b = V''(\phi_{eq})$. This is a damped simple harmonic oscillator equation and has the roots : $\alpha \equiv \frac{-a+\sqrt{a^2-4b}}{2}$ and $\beta \equiv \frac{-a-\sqrt{a^2-4b}}{2}$. Thus one gets the following solutions for ψ and $\dot{\psi}$:

$$\psi = Ae^{\alpha t} + Be^{\beta t} \tag{3.15}$$

$$\dot{\psi} = A\alpha e^{\alpha t} + B\beta e^{\beta t} \tag{3.16}$$

Now we can use the values of $\phi, \dot{\phi}$ at the equilibrium point as the initial conditions for this regime i.e. at $t = 0$, we have $(\phi, \dot{\phi}) = (\phi_{eq}, \dot{\phi}_{eq})$. Using this we get two equations and two unknowns solving which gives us the values of the constants A and B.

So how are equations (3.15)-(3.16) helpful? Let us take the example of a quadratic potential with $\phi_B = 1.06$. Suppose we already know $(\phi_{eq}, \dot{\phi}_{eq})$. Then it is straight forward to find the damping roots α, β. This gives us the evolution of $(\phi, \dot{\phi})$ in the form of (3.15)-(3.16). Now we can ask where does the inflaton turnaround i.e. when does $\dot{\phi} = 0$? We can put (3.16) to zero and solve for t and then plug this back into $(3.15) - (3.16)$ to get $\phi_{Turn} = 3.32$. Then we can go on to find the values of other observables like $H, \dot{H}$,etc at that point. Comparing with the numerical solutions given in Table 1 for $\phi_B = 1.06$, at the Turnaround point, the value of ϕ predicted by the analytics (3.15)-(3.16) is 3.32 while the numerics say it is 3.27 with percentage error being 1.53. Thus again we can trust these analytic solutions as they mimic the numerics. Other observables also behave in a similar way.

Now we need to discuss the reason why we ignored the KE with respect to the PE i.e. $V(\phi) \gg \frac{\dot{\phi}^2}{2}$ while retaining all the terms in the continuity equation. Again we can

use the definition of averages in (3.8) and compute them either numerically or analytically(using (3.15)-(3.16)), both of which agree. Let us first look at $\frac{<K>}{<V>}$ where $K = \dot{\phi}^2/2$ and $V = V(\phi)$. For all potentials its value is around 0.05 which means that on average the KE make up about only 5 percent of the total energy density. This justifies our assumptions. Also other ratios like $\langle K/V \rangle$ etc are small enough and thus again support our approximation. Now the ratio $\ddot{\phi} : 3H\dot{\phi} : V'$ is approximately $1 : 1 : 0.05$ for Starobinsky($\phi_B = 3.67$), $2.72 : 1.72 : 1$ for quadratic($\phi_B = 1.06$) and $2 : 2 : 1$ for quartic potential($\phi_B = 2.35$). As can be seen from this data, except for the Starobinsky potential, all terms in the continuity equation play an important role on average which justifies our retention of all the terms in the Continuity equation. It may seem reasonable to ignore the $V'(\phi)$-term in the Starobinsky case, but if we do that then the solution of equation (3.12) will be such that the inflaton will never go a turnaround and thus go through a subsequent phase of slow-roll. The fact the analytical and numerical solutions agree so well justifies the approximations we have used here.

Note that the solutions (3.15)-(3.18) can be over or under-damped depending on the value of ϕ_{eq}. For example, if ϕ_{eq} is close enough to the origin or is anywhere on the left side ($\phi < 0$) of the Starobinsky potential, then it might happen that $a^2 - 4b < 0$. Then the solution will automatically come out to be underdamped.

Where does this regime end? We choose to end it at the slow-roll point around which $\ddot{\phi} \approx 0$. This is not a very clear definition. So we define it as follows: The slow-roll point is the point where $\left|\frac{\ddot{\phi}}{3H\dot{\phi}}\right| = 0.01$ for the first time after the equilibrium point. This basically means that the $\ddot{\phi}$-term is ignorable with respect to other terms in the Continuity equation. It could also be understood as, since at the turnaround point η blows up, thus if there is a slow-roll regime in the future evolution then $|\eta| \sim |\frac{\ddot{\phi}}{3H\dot{\phi}}|$ should be small. This makes $|3H\dot{\phi}| \approx |V'|$.

One can ask why did we not choose the slow-roll point to be simply where $\ddot{\phi} = 0$. The answer to this is that there are cases like the Starobinsky potential with $\phi_B > 0$ where $\ddot{\phi}$ never vanishes because the damping equation (3.15) is such that $A < 0, B < 0, \alpha < 0, \beta > 0$ and this does not give us a point where $\ddot{\phi} = 0$. Similar behaviour can be seen in the numerics. One can say then that the slow-roll point can be where $\dddot{\phi} = 0$ (i.e. $|\ddot{\phi}|$ reaches its minimum) which will work for the above case but not in general. Thus it is best to define the slow-roll point as being the point where $\ddot{\phi}$ becomes about hundred times smaller that the friction and $V'(\phi)$ terms in the Continuity equation.

At this point the value of ϕ_{SRA} serves as initial condition for the Slow-Roll regime.

3.1.3 The Slow-Roll Regime

In this regime, we have three approximations: Firstly, $\rho \ll \rho_c$ as this regime comes after the damping regime where the density is also very low. Secondly, $\frac{\dot{\phi}^2}{2} \ll V(\phi)$. Thirdly, the slow-roll approximation(SRA) where we ignore the $\ddot{\phi}$ term in the continuity equation. Thus the basic equations here become :

$$H^2 \approx \frac{8\pi}{3}\rho \tag{3.17}$$

$$3H\dot{\phi} + V'(\phi) \approx 0 \tag{3.18}$$

$$\rho \approx V(\phi) \tag{3.19}$$

which are the standard slow-roll equations. We can eliminate the Hubble parameter and solve for $\dot{\phi}$ which gives us :

$$\dot{\phi} = \frac{-V'(\phi)}{\sqrt{24\pi V(\phi)}} \tag{3.20}$$

This is a first order differential equation which can be further integrated to get the evolution of ϕ as a function of time. This will introduce a constant of integration which can be fixed by using the value of ϕ_{SRA} got at the end of damping regime. Then we can estimate the value of observables at any point in the slow-roll regime like the star-point. Once we have the values of observables at the pivot point then we can determine if the inflaton has reached this point with the right conditions or not. If it has then the desired

slow-roll happens otherwise not. From the tables also it can be inferred that the numerics and analytics agree reasonably on the critical value of ϕ_B at/after which desired slow-roll starts.

Now we will discuss the reason why we ignored the KE with respect to the PE i.e. $\frac{\dot{\phi}^2}{2} \ll V(\phi)$ and ignored the $\ddot{\phi}$-term with respect to both the $3H\dot{\phi}$ and the $V'(\phi)$ terms in the continuity equation. Again we define averages as in (3.8) which can computed analytically and numerically. Let us first look at $\frac{<\dot{\phi}^2/2>}{<V(\phi)>}$ which is approximately 10^{-5} for Starobinsky and 10^{-3} for the quadratic/quartic potential which means that the Kinetic Energy on average makes up less than one percent of the total energy density and thus it is reasonable to ignore it. Also other ratios like $\left\langle K/V > \right.$ etc are very small and thus again support our approximation. Now the second ratio $< \ddot{\phi} >:< 3H\dot{\phi} >:< V' > \sim 10^{-\kappa} : 1 : 1$ where $\kappa = 3, 4, 5$ for Starobinsky, quadratic and quartic potentials respectively. This means that on average $V'(\phi)$ term and $< 3H\dot{\phi} >$ are comparable while the $\ddot{\phi}$ term is at least thousands of times smaller than them. This justifies why we ignore the $\ddot{\phi}$-term in the continuity equation.

It is important to note from all the Tables 1-6 that the desired slow-roll compatible with observations is achieved if and only if slow-roll starts before the pivot-point, and it is only in those cases do we apply (3.20) to get the values of observables at the star-point.

3.2 Potential Energy Domination at the Bounce

This corresponds to the case where $\frac{PE_B}{\rho_c} = F_B = f^2 \geq \frac{1}{2}$.

3.2.1 QG-assisted Damping Regime

Here the bounce is PE dominated and $\rho \approx V(\phi)$ i.e. the potential is comparable to the critical density. Thus this is a regime in which PE is dominating but quantum gravity effects also matter. So this regime is different from both the QG-assisted Kinetic regime and the damping regime of Sections 3.1.1 and 3.1.2. Thus we need a synthesis of approximations from both the regimes : Firstly, we will retain the holonomy correction term in the Friedmann equation as in (3.1). Secondly, we will ignore the KE with respect to the PE i.e. $\dot{\phi}^2 \ll V(\phi)$. Thirdly, we will retain all the terms in the Continuity equation. Thus the equations in this regime become:

$$H^2 = \frac{8\pi}{3}\rho\left(1 - \frac{\rho}{\rho_c}\right) \tag{3.21}$$

$$\ddot{\phi} + 3H\dot{\phi} + V'(\phi) = 0 \tag{3.22}$$

$$\rho \approx V(\phi) \tag{3.23}$$

Combining them and Taylor expanding $V'(\phi)$ to first order around $\phi = \phi_B$ and putting $V(\phi)$ as $V(\phi_B)$ as we did in Section 3.1.2, we again get a damped harmonic oscillator equation :

$$\ddot{\psi} + a\dot{\psi} + b\psi = 0 \tag{3.24}$$

where $a = \sqrt{24\pi V_B(1 - \frac{V_B}{\rho_c})}$ and $b = V''(\phi_B)$. Here $\psi = \phi + \frac{c}{b}$ where $c = V'(\phi_B) - \phi_B V''(\phi_B)$. Then the solutions will be as in (3.15)-(3.16) and the initial conditions required to determine the coefficients will be the conditions at the bounce i.e. $(\phi_B, \dot{\phi_B})$.

3.2.2 The Slow-Roll Regime

In this regime we have the following approximations: the slow-roll approximation demands $\ddot{\phi} \approx 0$, PE is dominant over KE thus $\rho \approx V(\phi)$ and since the slow-roll is very close to the bounce point, $V(\phi)$ is comparable to the critical density, thus we keep the quantum

gravity corrections as we did in (3.1). Thus the basic equations in this regime become:

$$H^2 = \frac{8\pi}{3}\rho\left(1 - \frac{\rho}{\rho_c}\right) \tag{3.25}$$

$$3H\dot{\phi} + V'(\phi) = 0 \tag{3.26}$$

$$\rho \approx V(\phi) \tag{3.27}$$

This leads us to :

$$\dot{\phi} = \frac{-V'(\phi)}{\sqrt{24\pi V(\phi)\left(1 - \frac{V(\phi)}{\rho_c}\right)}} \tag{3.28}$$

which can be integrated out to get an expression for ϕ as a function of time and thus other observables.

4 Comparison of Analytic and Numeric Data

4.1 Quadratic : $V(\phi) = \frac{1}{2}m^2\phi^2$

The quadratic potential is symmetric and thus has interesting observable features on both of its sides. Applying the procedure discussed in [23] i.e. using equations (2.10)-(2.15) we get the values of the mass parameter in the potential and also the necessary conditions at the pivot point compatible with observations as: $m = 1.21 \times 10^{-6} m_{Pl}$, $\phi_* = \pm 3.15 m_{Pl}$, $\dot{\phi}_* = \mp 1.97 \times 10^{-7} m_{Pl}^2$ and $\phi_{end} = 0.282 m_{Pl}$ just as in [20,21].

In all of our tables we have compared the data that comes out of our analytic and the published numerical methods. In Table 1, in each case the inflaton starts at the bounce with a huge amount of KE and the PE is negligible at the bounce. The picture is as follows: the inflaton starts at the bottom of the potential with positive velocity $\dot{\phi}_B = \sqrt{\rho_c - V(\phi_B)} \approx 9.05 \times 10^{-1}$ and moves up in the potential. Immediately it undergoes superinflation which ends at $\rho = \rho_c$ which according to (3.4) happens at $t = (24\pi\rho_c)^{-1/2} \approx 0.18$ Planck seconds after the bounce. This can be plugged into (3.5)-(3.6) to get the value of $(\phi, \dot{\phi})$ at the end of superinflation. Then the inflaton evolves and reassuringly

we see that the values of the observables like $\phi(t)$, $\dot{\phi}(t)$ etc are very close to the values obtained numerically. But because we are using approximations, the analytics will start differing from the numerics soon and the differences will be most prominent at the end of this phase i.e the equilibrium point. Perhaps an example will help. Let us take the fourth case of Table 1 i.e. $\phi_B = 1.06$ for which $f = 1.42 \times 10^{-6}$ at the bounce. Simply put $t = (24\pi\rho_c)^{-1/2} \approx 0.18 s_{Pl}$ into (3.5)-(3.6) to get $(\phi, \dot{\phi}) = (1.20, 6.40 \times 10^{-1})$ which completely agrees with the numerics. Next we use equation (3.7) to find the time at which KE=PE. We first simplified this expression for the quadratic potential and then used Mathematica to solve for t for $\phi_B = 1.06$:

$$\frac{1.346 * 10^5}{t} = 1.06 + (0.163) * \log[11.12t] \tag{4.1}$$

where in the above we have used a natural logarithm. Solving this we get $t_{eq} = 4.22 \times 10^4$ which when used in (3.5)-(3.6) we get $(\phi, \dot{\phi}) = (3.19, 3.86 \times 10^{-6})$ which again agrees very well with the numerics. These values serve as the initial conditions for the damping phase. However the analytics and published numerics don't agree exactly on the time it takes to reach equilibrium point. The numerics say $t_{eq} = 3.73 \times 10^4$ which leads to 13 percent error. In general for all the potentials we have considered both the primary and secondary estimates are within a percent or so and the estimates in time are greater than ten percent. We believe the primary and secondary observables are the key ones.

According to the discussion in (3.1.2) we get $a = \sqrt{24\pi V_{eq}} = m\sqrt{12\pi}\phi_{eq} = 2.36774 \times 10^{-5}$ and $b = V''(\phi_{eq}) = 1.4641 \times 10^{-12}$. Using these we get the damping roots as $\frac{-a \pm \sqrt{a^2 - 4b}}{2} = (\alpha, \beta) = (-2.36 \times 10^{-5}, -6.20 \times 10^{-8})$. Now we will use (3.15)-(3.16) and the equilibrium values of observables as initial conditions to get the values of $(A, B) = (-0.172, 3.36)$ and thus the damping equations as :

$$\phi = (-0.172)e^{-2.36 \times 10^{-5} t} + (3.36)e^{-6.20 \times 10^{-8} t} \tag{4.2}$$

and differentiating this we get $\dot{\phi}$. We can ask when does turnaround happen i.e. when does $\dot{\phi}(t) = 0$? We can differentiate (4.2) and set it to zero to obtain $t = 1.26151 \times 10^5$ and then

put it back in (4.2) which gives $\phi_{Turn} = 3.32$ whereas numerics give us $\phi_{Turn} = 3.27$ and thus they are in good agreement. Also the above time is not the total time as this t starts from the equilibrium point and thus we need to add t_{eq} which gives $t_{Turn} = 1.68 \times 10^5$.

Now for the slow-roll point we ask the following question: since damping starts at what time does the inflaton first satisfy the condition $\left|\frac{\ddot{\phi}}{3H\dot{\phi}}\right| = 0.01$? We can solve this in Mathematica to get t which when used with (4.2) gives us $(\phi, \dot{\phi}) = (3.31, -1.95 \times 10^{-7})$ as opposed to numerics which give $(3.25, -1.95 \times 10^{-7})$ with respective percent errors $(1.85, 0)$. Actually $\frac{\ddot{\phi}}{3H\dot{\phi}}$ can be ± 0.01. It turns out that for Table 1 both in numerical and analytic cases $\frac{\ddot{\phi}}{3H\dot{\phi}} = 0.01$ marks the beginning of slow-roll whereas for Table 2 it is the other sign. It is remarkable that our analytics don't just predict nearly correct values for the observables but they also mimic the overall physical features. Another physical feature that is mimicked by these analytics is the point where $\ddot{\phi} = 0$. Such a point exists for Table 1 cases but not for Table 2 and the analytics and numerics both agree upon this fact. This is the reason why we chose not to define the beginning of slow-roll as a point where $\ddot{\phi} = 0$ as this is not universal behaviour.

For the slow-roll regime we first ask does the inflaton reach the slow-roll point before reaching the pivot point? If yes then the desired slow-roll compatible with observations (2.10)-(2.15) will happen and then we apply (3.20). For $\phi_B = 1.06$ we got $\phi_{SRA} = 3.31 > \phi_* = 3.15$ thus at the pivot point the inflaton velocity is given by (3.20) as $\dot{\phi} = -m/\sqrt{12\pi} = -1.97 \times 10^{-7}$. (3.20) can be used to find time t taken from slow-roll point to the pivot point which when added to t_{SRA} gives you the total time from bounce till pivot point $t_* = 1.11 \times 10^6$ as opposed to the numerics which give $t_* = 8.33 \times 10^5$. For Table 2 cases, the procedure is very similar except now the inflaton simply starts rolling down the hill from the beginning and thus after the equilibrium point never turns around and hits the slow-roll directly. Here again the analytics agree with the published numerics to within a percent or so.

How do we calculate the secondary observables? Let us consider two of them: the Hubble parameter H and $\ddot{\phi}$ defined in (2.1) and (2.9) respectively. H requires knowledge of the total energy density $\rho = KE + PE = \frac{\dot{\phi}^2}{2} + V(\phi)$. Whenever we derive analytic formulas like (3.5)-(3.6) we used the approximation of neglecting the PE in ρ. But once we have (3.5)-(3.6) we will take $\rho = KE + PE$ as this will give us the right results up to the equilibrium point. So (3.4) is only valid for points very close to the bounce. Also if we want $\dot{H}$ then we differentiate (2.1) to get (2.4) and so on for rest of the observables. What about $\ddot{\phi}$? Numerically it can be defined as both $\frac{d\dot{\phi}}{dt}$ or $-3H\dot{\phi} - V'(\phi)$? But for analytics the two quantities can differ because of our use of approximations. The first definition leads to an appreciable discontinuity at the equilibrium point in the values of $\ddot{\phi}$, $\dot{\eta}$ etc. These discontinuities can affect the solutions of Mukhanov-Sasaki equation $\chi_k'' + (k^2 - \frac{z''}{z})\chi_k = 0$ where $'$ denotes differentiation with respect to the conformal time and $z = a\dot{\phi}/H$. Thus it might lead to extra features in the CMB which are not seen today. The reason why $\ddot{\phi}$ becomes discontinuous at the equilibrium point is essentially because differentiating (3.5) leads to $\ddot{\phi} = -3H\dot{\phi}$ i.e. without any $V'(\phi)$-term as expected from the approximations, whereas differentiating (3.16) takes the $V'(\phi)$-term into account. However the second definition smoothly connects the two regimes at the equilibrium point because $-3H\dot{\phi} - V'(\phi)$ is a function of $(\phi, \dot{\phi})$ only which are exactly the same at the equilibrium point as they are initial conditions for the damping regime. Thus this is also the definition we use when we have to find the slow-roll point. All this discussion about secondary observables is true for all potentials.

One important thing to note from Tables 1 and 2 is the difference in predictions for the critical point i.e the value of ϕ_B after which all intital conditions at the bounce lead to the desired slow-roll. For Table 1 the critical point is 0.898 numerically and 0.961. For Table 2 the critical point is -5.47 numerically and -5.44. This difference comes again because of the approximations used to get analytic solutions which is expected. However

the aim of these analytics is not to match everything precisely with the numerics, rather what we want is to mimic the general behaviour of primary and secondary observables so that they can be used with confidence in the study of perturbations, in particular derive the interesting results of [19] and [22,23] i.e. power suppression for large angular scales of CMB and the possibility of linking these with non-gaussianity.

In these tables we have not shown any PE dominated cases because there the inflaton hardly evolves from the bounce point to turnaround to the slow-roll point. What we mean is that if we start at $\phi_B = 6 \times 10^5$ then say at the turnaround point we will have $\phi_{Turn} = \phi_B + 1.00$ which is a change of 1.7×10^{-4} percent. Thus the inflaton hardly moves and this agrees with the numerics as is discussed in [20,21].

Event	ϕ_A	$\dot{\phi_A}$	t_A	ϕ_N	$\dot{\phi_N}$	t_N
Bounce	8.00×10^{-1}	9.05×10^{-1}	0	8.00×10^{-1}	9.05×10^{-1}	0
End of SI	9.43×10^{-1}	6.40×10^{-1}	1.80×10^{-1}	9.43×10^{-1}	6.40×10^{-1}	1.80×10^{-1}
KE = PE	2.94	3.56×10^{-6}	4.58×10^{4}	2.91	3.52×10^{-6}	4.04×10^{4}
Turn	3.08	0	1.79×10^{5}	3.03	0	1.65×10^{5}
Slow-Roll	3.06	-1.95×10^{-7}	3.15×10^{5}	2.99	-1.95×10^{-7}	3.71×10^{5}
$*$	NA	NA	NA	NA	NA	NA
Bounce	8.98×10^{-1}	9.05×10^{-1}	0	8.98×10^{-1}	9.05×10^{-1}	0
End of SI	1.04	6.40×10^{-1}	1.80×10^{-1}	1.04	6.40×10^{-1}	1.80×10^{-1}
KE = PE	3.03	3.67×10^{-6}	4.44×10^{4}	3.00	3.63×10^{-6}	3.91×10^{4}
Turn	3.17	0	1.75×10^{5}	3.12	0	1.62×10^{5}
Slow-Roll	3.15	-1.95×10^{-7}	3.08×10^{5}	3.09	-1.95×10^{-7}	3.61×10^{5}
$*$	3.15	-1.97×10^{-7}	3.11×10^{5}	NA	NA	NA
Bounce	9.61×10^{-1}	9.05×10^{-1}	0	9.61×10^{-1}	9.05×10^{-1}	0
End of SI	1.10	6.40×10^{-1}	1.80×10^{-1}	1.10	6.40×10^{-1}	1.80×10^{-1}
KE = PE	3.09	3.74×10^{-6}	4.35×10^{4}	3.06	3.70×10^{-6}	3.84×10^{4}
Turn	3.23	0	1.72×10^{5}	3.18	0	1.59×10^{5}
Slow-Roll	3.21	-1.95×10^{-7}	3.03×10^{5}	3.15	-1.95×10^{-7}	3.55×10^{5}
$*$	3.15	-1.97×10^{-7}	6.13×10^{5}	3.15	-1.95×10^{-7}	3.56×10^{5}
Bounce	1.06	9.05×10^{-1}	0	1.06	9.05×10^{-1}	0
End of SI	1.20	6.40×10^{-1}	1.80×10^{-1}	1.20	6.40×10^{-1}	1.80×10^{-1}
KE = PE	3.19	3.86×10^{-6}	4.22×10^{4}	3.16	3.82×10^{-6}	3.73×10^{4}
Turn	3.32	0	1.68×10^{5}	3.27	0	1.56×10^{5}
Slow-Roll	3.31	-1.95×10^{-7}	2.96×10^{5}	3.25	-1.95×10^{-7}	3.46×10^{5}
$*$	3.15	-1.97×10^{-7}	1.11×10^{6}	3.15	-1.97×10^{-7}	8.33×10^{5}

Table 1: Comparison of Analytic(A) and Numeric(N) data for the evolution of observables for KE dominated cases with $\phi_B > 0$ for a quadratic potential, $V(\phi) = \frac{1}{2}m^2\phi^2$ where $m = 1.21 \times 10^{-6}$. Each block represents an initial condition at the bounce and each row within a block represents an event in ascending order: Bounce, End of Superinflation, Equilibrium, Turnaround, Slow-roll and Pivot point. The desired slow-roll happens $\phi_B \geq 0.898$ for analytics and $\phi_B \geq 0.961$ for numerics.

Event	ϕ_A	$\dot{\phi_A}$	t_A	ϕ_N	$\dot{\phi_N}$	t_N
Bounce	-5.40	9.05×10^{-1}	0	-5.40	9.05×10^{-1}	0
End of SI	-5.26	6.40×10^{-1}	1.80×10^{-1}	-5.26	6.40×10^{-1}	1.80×10^{-1}
KE = PE	-3.28	3.97×10^{-6}	4.11×10^{4}	-3.31	4.00×10^{-6}	3.62×10^{4}
Slow-Roll	-3.08	1.99×10^{-7}	2.74×10^{5}	-3.11	1.99×10^{-7}	3.47×10^{5}
$*$	NA	NA	NA	NA	NA	NA
Bounce	-5.44	9.05×10^{-1}	0	-5.44	9.05×10^{-1}	0
End of SI	-5.30	6.40×10^{-1}	1.80×10^{-1}	-5.30	6.40×10^{-1}	1.80×10^{-1}
KE = PE	-3.32	4.02×10^{-6}	4.05×10^{4}	-3.35	4.05×10^{-6}	3.57×10^{4}
Slow-Roll	-3.12	1.99×10^{-7}	2.71×10^{5}	-3.15	1.99×10^{-7}	3.43×10^{5}
$*$	NA	NA	NA	-3.15	1.98×10^{-7}	3.57×10^{5}
Bounce	-5.47	9.05×10^{-1}	0	-5.47	9.05×10^{-1}	0
End of SI	-5.33	6.40×10^{-1}	1.80×10^{-1}	-5.33	6.40×10^{-1}	1.80×10^{-1}
KE = PE	-3.35	4.05×10^{-6}	4.02×10^{4}	-3.38	4.09×10^{-6}	3.54×10^{4}
Slow-Roll	-3.15	1.99×10^{-7}	2.70×10^{5}	-3.18	1.99×10^{-7}	3.40×10^{5}
$*$	-3.15	1.97×10^{-7}	2.85×10^{5}	-3.15	1.97×10^{-7}	5.17×10^{6}
Bounce	-5.50	9.05×10^{-1}	0	-5.50	9.05×10^{-1}	0
End of SI	-5.36	6.40×10^{-1}	1.80×10^{-1}	-5.36	6.40×10^{-1}	1.80×10^{-1}
KE = PE	-3.38	4.09×10^{-6}	3.98×10^{4}	-3.41	4.13×10^{-6}	3.51×10^{4}
Slow-Roll	-3.18	1.99×10^{-7}	2.68×10^{5}	-3.22	1.99×10^{-7}	3.38×10^{5}
$*$	-3.15	1.97×10^{-7}	4.20×10^{5}	-3.15	1.97×10^{-7}	6.76×10^{5}

Table 2: Comparison of Analytic(A) and Numeric(N) data for the evolution of observables for KE dominated cases with $\phi_B < 0$ for a quadratic potential, $V(\phi) = \frac{1}{2}m^2\phi^2$ where $m = 1.21 \times 10^{-6}$. Each block represents an initial condition at the bounce and each row within a block represents an event in ascending order: Bounce, End of Superinflation, Equilibrium, Turnaround, Slow-roll and Pivot point. The desired slow-roll happens $\phi_B \leq -5.47$ for analytics and $\phi_B \leq -5.44$ for numerics

4.2 Starobinsky : $V(\phi) = \frac{3M^2}{32\pi}\left(1 - e^{-\sqrt{\frac{16\pi}{3}}\phi}\right)^2$

The Starobinsky potential is not a symmetric potential. Close to the origin it behaves as a quadratic and for large positive values of phi it asymptotes to a constant. Thus it has interesting observable features. Applying the procedure discussed in [23] i.e. using equations (2.10)-(2.15) we get the values of the mass parameter in the potential and also the necessary conditions at the pivot point compatible with observations as: $M = 2.51 \times 10^{-6} m_{Pl}$, $\phi_* = 1.08 m_{Pl}$, $\dot{\phi}_* = -4.80 \times 10^{-9} m_{Pl}^2$ and $\phi_{end} = 0.187 m_{Pl}$ just as in [23].

In all of our tables we have compared the data that comes out of analytic and numerical methods. In Table 3, in each case the inflaton starts at the bounce with a huge amount of KE and the PE is negligible at the bounce. The picture is as follows: the inflaton starts at the bottom of the potential with positive velocity $\dot{\phi}_B = \sqrt{\rho_c - V(\phi_B)} \approx 9.05 \times 10^{-1}$ and moves up in the potential. Immediately it undergoes superinflation ending at $\rho = \rho_c$ which according to (3.4) happens at $t = (24\pi\rho_c)^{-1/2} \approx 0.18$ Planck seconds. This can be plugged into (3.5)-(3.6) to get the value of $(\phi, \dot{\phi})$ at the end of superinflation. Then the inflaton evolves and the value of the observables like $\phi(t)$, $\dot{\phi}(t)$ etc that we obtain are seen to be very close to the numerical values.The agreement between the analytic and numerical solutions eventually begins to break down as the assumptions that have gone into the analytic calculations become invalid. It begins to happen generally around the equilibrium point. For example let us take the fourth case of Table 3 i.e. $\phi_B = -1.37$. We initially put $t = (24\pi\rho_c)^{-1/2} \approx 0.18 s_{Pl}$ into (3.5)-(3.6) to get $(\phi, \dot{\phi}) = (-1.23, 6.40 \times 10^{-1})$ which completely agrees with the numerical results. Next we use equation (3.7) to find the time at which the KE=PE. We first simplified this expression for the Starobinsky potential and then used Mathematica to solve for t with $\phi_B = -1.37$:

$$\frac{2.66 \times 10^5}{t} = [1 - e^{-\sqrt{\frac{16\pi}{3}} \times -1.37}(11.12t)^{-2/3}] \tag{4.3}$$

Solving this we get $t_{eq} = 2.67 \times 10^5$ which when used in (3.5)-(3.6) yields $(\phi, \dot{\phi}) = (1.06, 6.09 \times 10^{-7})$ which again agrees very well with the numerical solutions. However

they don't agree exactly on the time it takes to reach equilibrium point. The numerics say $t_{eq} = 2.37 \times 10^5$ which leads to 13 percent error which is still very good. These values serve as the initial conditions for the damping phase.

According to the discussion in (3.1.2) we get $a = \sqrt{24\pi V_{eq}} = 3.71537 \times 10^{-6}$ and $b = V''(\phi_{eq}) = -8.08566 \times 10^{-14}$. Using these we get the damping roots as $\frac{-a \pm \sqrt{a^2-4b}}{2} = (\alpha, \beta) = (-3.74 \times 10^{-6}, 2.16 \times 10^{-8})$. Now we will use (3.15)-(3.16) and the equilibrium values of observables as initial conditions to get the values of $(A, B) = (-0.163, -0.0841)$ and thus the damping solution for ϕ as :

$$\phi = (-0.163)e^{-3.74\times10^{-6}t} + (-0.0841)e^{2.16\times10^{-8}t} + 1.30 \tag{4.4}$$

and differentiating this we get $\dot{\phi}$. We can ask when does turnaround happen i.e. when does $\dot{\phi}(t) = 0$? We can simply solve this using (4.2) for $t = 1.26 \times 10^5$ and then substitute it back in (4.4) which gives $\phi_{Turn} = 1.22$ whereas numerics give us $\phi_{Turn} = 1.17$ and thus they are within 4 percent of each other. Also the above time is not the total time as this t starts from the equilibrium point and thus we need to add t_{eq} which gives $t_{Turn} = 1.81 \times 10^6$.

Now for the slow-roll point we ask the following question: since damping starts at what time does the inflaton first satisfy the condition $\left|\frac{\ddot{\phi}}{3H\dot{\phi}}\right| = 0.01$? We can solve this in Mathematica to get t which when used with (4.4) gives us $(\phi, \dot{\phi}) = (1.08, -4.81 \times 10^{-9})$ as opposed to numerics which give $(1.16, -3.48 \times 10^{-9})$ (three seems to be a lot of difference in inflaton velocities which we will explain below). Actually $\frac{\ddot{\phi}}{3H\dot{\phi}}$ can be ± 0.01. It turns out that for Table 3 both in numerical and analytic cases $\frac{\ddot{\phi}}{3H\dot{\phi}} = 0.01$ marks the beginning of slow-roll whereas for Table 4 it is the other sign. Just as we said with the quadratic potentials in section 2, it is remarkable that here as well we see that our analytical solutions mimic the numerical solutions.

For the slow-roll regime we first ask does the inflaton reach the slow-roll point be-

fore reaching the pivot point? If yes then the desired slow-roll compatible with observations (2.10)-(2.15) will happen and then we apply (3.20). For $\phi_B = -1.37$ we got $\phi_{SRA} = 1.08 = \phi_* = 3.15$ thus at the pivot point the inflaton velocity is given by (3.20) as $\dot{\phi} = -M/\sqrt{12\pi}e^{-\sqrt{16\pi/3}\phi_*} = -4.92 \times 10^{-9}$. (3.20) can be used to find the time t taken from the slow-roll point to the pivot point which when added to t_{SRA} gives the total time from bounce till pivot point $t_* = 4.58 \times 10^7$ as opposed to the numerics which give $t_* = 2.28 \times 10^7$. For Table 4 cases, the procedure is very similar except now the inflaton simply starts rolling down the hill from the beginning and thus after the equilibrium point never turns around and hits the slow-roll directly. There too the analytic procedure is similar and mimics the numerical solutions to within a few percent.

One important thing to note from Tables 3 and 4 is the difference in predictions for the critical point i.e the value of ϕ_B after which all intital conditions at the bounce lead to the desired slow-roll. For Table 3 the critical point is -1.45 numerically and -1.37 analytically. For Table 4 the critical point is 3.63 numerically and 3.68 analytically. The fact that they are no more than 5 percent is testament to the accuracy of the analytic solutions.

Now let us discuss the PE dominated cases. In Table 3 and 4 we have the cases $\phi_B = -3.47$ and $\phi_B = -3.39$. In principle we should be applying the techniques discussed in section 3.2 and 3.3. But these are not very helpful in deciding whether they will lead to desired slow-roll or not. We introduce a new approach to determining the solutions in this regime. Let us start with $\phi_B = -3.47$. We can use QG-assisted damping (3.24) here to find when does superinflation end i.e. when does $\rho(t) = 0.41/2$. Once this is found then the value of t can be substituted back into (3.24) to obtain $(\phi, \dot{\phi}) = (-3.28, 0.484)$ while the numerical results say $(-3.25, 0.520)$ which are accurate to 1 and 7 percent respectively. Now we introduce the new approach:

1. At $\phi_B = -3.28$ the potential can be accurately approximated by $V(\phi) = \frac{3M^2}{32\pi}\big(1 -$

$e^{-\sqrt{\frac{16\pi}{3}}\phi}\big)^2 \approx V_0 e^{-2b\phi}$ where $V_0 = \frac{3M^2}{32\pi}$ and $b = -\sqrt{\frac{16\pi}{3}}$

2. Here we introduce an ansatz $\dot{\phi} = \gamma e^{-b\phi}$ where γ is a constant. This ansatz can be checked to be approximately true numerically for points at the end of superinflation, equilibrium point etc and also there are mathematical reasons for this choice which we will explain soon.

3. Within $10 - 20$ Planck seconds the total energy density becomes negligible with respect to the critical density $\rho \ll \rho_c$. Thus the Hubble parameter can be written as $H = \sqrt{\frac{8\pi V_0}{3}} e^{-b\phi} \sqrt{1 + \frac{c^2}{2V_0}}$ and the continuity equation becomes

$$\ddot{\phi} + 3\sqrt{\frac{8\pi V_0}{3}} \sqrt{1 + \frac{\dot{\phi}^2}{2V(\phi)}} e^{-b\phi}\dot{\phi} - 2bV_0 e^{-2b\phi} = 0 \tag{4.5}$$

We can see that $\ddot{\phi}$, $e^{-b\phi}\dot{\phi}$ and the third term can all be made equivalent to each other if we choose the above ansatz. As a result the square root term containing the ratio KE and PE can also be simplified as $\sqrt{1 + \frac{\gamma^2}{2V_0}}$. Thus cancelling out all $e^{-2b\phi}$ we get an equation in terms of γ:

$$-\gamma^2 b + \sqrt{24\pi V_0} \sqrt{1 + \frac{\gamma^2}{2V_0}} \gamma - 2bV_0 = 0 \tag{4.6}$$

which can be solved to give $\gamma = 5.48 \times 10^{-7}$. Now we can solve $\dot{\phi} = \gamma e^{-b\phi}$ to get analytic expressions for $(\phi, \dot{\phi})$ which can be substituted into $\dot{\phi}^2/2 = V(\phi)$ to get the value of t where equilibrium happens which then can be put back into the analytic expressions to get $(\phi_{eq}, \dot{\phi}_{eq})$. Doing this we obtain $(\phi_{eq}, \dot{\phi}_{eq}) = (-0.55, 5.19 \times 10^{-6})$ which is remarkably close to the exact numerical solutions $(-0.55, 5.14 \times 10^{-6})$. We can extrapolate this solution to the origin by simply putting $\phi = 0$ in $\dot{\phi}_o = \gamma e^{-b\phi} = \gamma$. Thus when the inflaton reaches the origin it only has KE and we can use the same techniques as discussed in (3.1.1) the only difference is that now $\rho \ll \rho_c$. Thus the solution will be:

$$\phi = \frac{1}{\sqrt{12\pi}} \log[1 + \sqrt{12\pi}\gamma t] \tag{4.7}$$

We can now use this to get the values of our observables at a second equilibrium point as

shown in Table 3. The values of the observables obtained from the analytical solutions for the second equilibrium point are $(\phi, \dot{\phi}) = (0.128, 2.50 \times 10^{-7})$ as opposed to the numerical result $(0.093, 1.93 \times 10^{-7})$ with respective percent errors $(38, 30)$. Next we use the usual damping solutions discussed in (3.1.2) to go from $\phi = 0.128$ to $\phi = 0.132$ which for this range are under-damped. Once we reach $\phi = 0.132$ we then again apply the damping solution (which is now over-damped) until the inflaton reaches a turnaround at $\phi = 0.337$ (while the numerics say $\phi = 0.127$) and thus cannot slow-roll near $\phi_* = 1.08$. Thus we stop our solution as this is not going to lead to the desired slow-roll which agrees with the numerical result.

In Table 4 we start at $\phi_B = -3.39$ with negative velocity i.e. we are going uphill. The maximum height allowed is $\phi = -3.47$ which is found by equating the Starobinsky potential to the critical energy density. If we use our usual damping solutions (3.24) then the turnaround happens at $\phi = -3.52$ which cannot be allowed. To address this discrepancy we modify the approach taken above:

1. The Hubble parameter is always zero at the bounce and while going uphill the inflaton turns around and thus $\dot{\phi} = 0$. Numerically it can be seen that for the first few planck seconds (equals $\sqrt{\frac{\hbar G}{c^5}} = 5.39 \times 10^{-44}$ seconds) the friction term $3H\dot{\phi}$ is close to zero while the other terms in the continuity equation are large.

2. Again we can say that at $\phi_B = -3.39$ the potential is well approximated by $V(\phi) = \frac{3M^2}{32\pi}\left(1 - e^{-\sqrt{\frac{16\pi}{3}}\phi}\right)^2 \approx V_0 e^{-2b\phi}$ where $V_0 = \frac{3M^2}{32\pi}$ and $b = -\sqrt{\frac{16\pi}{3}}$

3. The continuity equation can then be integrated out leading to our new modified solution:

$$\dot{\phi} = -\sqrt{2\rho_c - 2V_0 e^{-2b\phi}} \tag{4.8}$$

which can then be integrated yielding analytic expressions for $(\phi, \dot{\phi})$. Then we obtain the

turnaround at $\phi = -3.47$ as opposed to the numerical result $\phi = -3.46$ which is an error of 0.3 percent. Then we extend this solution further and stop it at a point $\phi = -3.40$ where the numerics say that our approximation $3H\dot{\phi} \approx 0$ does not hold any more. But at this point $\dot{\phi}e^{b\phi} = 5.46 \times 10^{-7}$ which basically is $\gamma = 5.48 \times 10^{-7}$ derived in (4.6). So now we can use the same approach as discussed in (4.5)-(4.7) and again we conclude that the desired slow-roll does not happen here, an analytic prediction which matches with the numerical solution. So in general for PE dominated cases of Starobinsky potential we don't get desired slow-roll.

Event	ϕ_A	$\dot{\phi_A}$	t_A	ϕ_N	$\dot{\phi_N}$	t_N
Bounce	-3.47	5.07×10^{-2}	0	-3.47	5.07×10^{-2}	0
End of SI	-3.28	4.84×10^{-1}	0.41	-3.25	5.20×10^{-1}	0.46
KE = PE	-0.55	5.19×10^{-6}	4.70×10^{4}	-0.55	5.14×10^{-6}	4.70×10^{4}
Origin	0	5.48×10^{-7}	4.45×10^{5}	0	4.62×10^{-7}	4.68×10^{5}
KE=PE	0.128	2.50×10^{-7}	3.54×10^{5}	0.093	1.93×10^{-7}	7.64×10^{-7}
Turn	0.337	0	7.42×10^{5}	0.127	0	1.15×10^{6}
$*$	NA	NA	NA	NA	NA	NA
Bounce	-1.45	9.05×10^{-1}	0	-1.45	9.05×10^{-1}	0
End of SI	-1.31	6.40×10^{-1}	1.80×10^{-1}	-1.31	6.40×10^{-1}	1.80×10^{-1}
KE = PE	0.98	6.08×10^{-7}	2.68×10^{5}	0.95	6.01×10^{-7}	2.38×10^{5}
Turn	1.14	0	1.73×10^{6}	1.08	0	1.49×10^{6}
Slow-Roll	1.00	-6.80×10^{-9}	4.30×10^{6}	1.08	-4.88×10^{-9}	2.91×10^{6}
$*$	NA	NA	NA	1.08	-4.85×10^{-9}	2.76×10^{6}
Bounce	-1.41	9.05×10^{-1}	0	-1.41	9.05×10^{-1}	0
End of SI	-1.27	6.40×10^{-1}	1.80×10^{-1}	-1.27	6.40×10^{-1}	1.80×10^{-1}
KE = PE	1.02	6.08×10^{-7}	2.68×10^{5}	0.99	6.02×10^{-7}	2.38×10^{5}
Turn	1.18	0	1.77×10^{6}	1.12	0	1.53×10^{6}
Slow-Roll	1.04	-5.71×10^{-9}	3.88×10^{7}	1.12	-4.12×10^{-9}	2.92×10^{6}
$*$	NA	NA	NA	1.08	-4.89×10^{-9}	1.20×10^{7}
Bounce	-1.37	9.05×10^{-1}	0	-1.37	9.05×10^{-1}	0
End of SI	-1.23	6.40×10^{-1}	1.80×10^{-1}	-1.23	6.40×10^{-1}	1.80×10^{-1}
KE = PE	1.06	6.09×10^{-7}	2.67×10^{5}	1.03	6.04×10^{-7}	2.37×10^{5}
Turn	1.22	0	1.81×10^{6}	1.17	0	1.57×10^{6}
Slow-Roll	1.08	-4.81×10^{-9}	4.52×10^{7}	1.16	-3.48×10^{-9}	2.93×10^{7}
$*$	1.08	-4.92×10^{-9}	4.58×10^{7}	1.08	-4.89×10^{-9}	2.28×10^{7}

Table 3: Comparison of Analytic(A) and Numeric(N) data for the evolution of observables with $\dot{\phi}_B > 0$ for Starobinsky potential. The last three blocks are KE dominated cases wherein each row represents an event in ascending order: Bounce, End of Superinflation, Equilibrium, Turnaround, Slow-roll and Pivot point. The first row is PE dominated case with more events. The desired slow-roll happens $\phi_B \geq -1.37$ (analytics) and $\phi_B \geq -1.45$

Event	ϕ_A	$\dot{\phi_A}$	t_A	ϕ_N	$\dot{\phi_N}$	t_N
Bounce	-3.39	-6.29×10^{-1}	0	-3.39	-6.29×10^{-1}	0
Turn	-3.47	0	2.31×10^{-1}	-3.46	0	2.18×10^{-1}
Stop New-Ed	-3.40	6.04×10^{-1}	4.48×10^{-1}	-3.40	4.95×10^{-1}	4.39×10^{-1}
KE = PE	-0.55	5.19×10^{-6}	4.70×10^{4}	-0.55	5.14×10^{-6}	4.70×10^{4}
Origin	0	5.48×10^{-7}	4.45×10^{5}	0	4.62×10^{-7}	4.68×10^{5}
KE=PE	0.128	2.50×10^{-7}	3.54×10^{5}	0.093	1.93×10^{-7}	7.64×10^{5}
Turn	0.337	0	7.42×10^{5}	0.127	0	1.15×10^{6}
$*$	NA	NA	NA	NA	NA	NA
Bounce	3.63	-9.05×10^{-1}	0	3.63	-9.05×10^{-1}	0
End of SI	3.49	-6.40×10^{-1}	1.80×10^{-1}	3.49	-6.40×10^{-1}	1.80×10^{-1}
KE = PE	1.20	-6.09×10^{-7}	2.67×10^{5}	1.23	-6.09×10^{-7}	2.36×10^{5}
Slow-Roll	1.03	-6.02×10^{-9}	1.97×10^{6}	1.08	-4.97×10^{-9}	2.59×10^{6}
$*$	NA	NA	NA	1.08	-4.97×10^{-9}	2.58×10^{7}
Bounce	3.67	-9.05×10^{-1}	0	3.67	-9.05×10^{-1}	0
End of SI	3.53	-6.40×10^{-1}	1.80×10^{-1}	3.53	-6.40×10^{-1}	1.80×10^{-1}
KE = PE	1.24	-6.09×10^{-7}	2.67×10^{5}	1.27	-6.10×10^{-7}	2.35×10^{5}
Slow-Roll	1.07	-5.09×10^{-9}	2.03×10^{6}	1.12	-4.19×10^{-9}	2.64×10^{6}
$*$	NA	NA	NA	1.08	-4.89×10^{-9}	1.19×10^{7}
Bounce	3.68	-9.05×10^{-1}	0	3.68	-9.05×10^{-1}	0
End of SI	3.54	-6.40×10^{-1}	1.80×10^{-1}	3.54	-6.40×10^{-1}	1.80×10^{-1}
KE = PE	1.25	-6.10×10^{-7}	2.67×10^{5}	1.28	-6.10×10^{-7}	2.35×10^{5}
Slow-Roll	1.08	-4.88×10^{-9}	2.03×10^{6}	1.13	-4.02×10^{-9}	2.66×10^{6}
$*$	1.08	-4.92×10^{-9}	2.90×10^{6}	1.08	-4.89×10^{-9}	1.44×10^{7}

Table 4: Comparison of Analytic(A) and Numeric(N) data for the evolution of observables for the case $\dot{\phi}_B < 0$ for Starobinsky potential. The last three blocks are KE dominated cases wherein each row represents an event in ascending order: Bounce, End of Superinflation, Equilibrium, Turnaround, Slow-roll and Pivot point. The first row is PE dominated case with similar timeline and does not lead to desired slow-roll. The desired slow-roll happens $\phi_B \geq 3.68$ for analytics and $\phi_B > 3.63$ for numerics.

4.3 Quartic : $V(\phi) = \lambda\phi^4$

The quartic potential is similar to the quadratic potential. Applying the procedure discussed in [23] i.e. using equations (2.10)-(2.15) we get the values of the mass parameter in the potential and also the necessary conditions at the pivot point compatible with observations as: $\lambda = 3.97 \times 10^{-14}$, $\phi_* = \pm 4.406 m_{Pl}$, $\dot{\phi}_* = \mp 4.03 \times 10^{-7} m_{Pl}^2$ and $\phi_{end} = 0.5642 m_{Pl}$.

In Table 5, in each case the inflaton starts at the bounce with a huge amount of KE and the PE is negligible at the bounce. The picture is as follows: the inflaton starts at the bottom of the potential with positive velocity $\dot{\phi}_B = \sqrt{\rho_c - V(\phi_B)} \approx 9.05 \times 10^{-1}$ and moves up in the potential. Immediately it undergoes superinflation which ends at $\rho = \rho_c$ which according to (3.4) happens at $t = (24\pi\rho_c)^{-1/2} \approx 0.18 s_{Pl}$. This can be plugged into (3.5)-(3.6) to get the value of $(\phi, \dot{\phi})$ at the end of superinflation. Then the inflaton evolves and the value of the observables like $\phi(t)$, $\dot{\phi}(t)$ etc are very close to the numerics. But because we are using approximations, the analytics will start differing from the numerics soon and the differences will be most prominent at the end of this phase i.e the equilibrium point. Let us take the fourth case of Table 5 i.e. $\phi_B = 2.35$. Simply put $t = (24\pi\rho_c)^{-1/2} \approx 0.18 s_{Pl}$ into (3.5)-(3.6) to get $(\phi, \dot{\phi}) = (2.49, 6.40 \times 10^{-1})$ which completely agrees with the numerics. Next we use equation (3.7) to find the time at which KE=PE. We first simplified this expression for the quartic potential and then used Mathematica to solve for t for $\phi_B = 2.35$:

$$\frac{760}{\sqrt{t}} = 2.35 + (0.163) * \log[11.12t] \tag{4.9}$$

where in the above we have used a natural logarithm. Solving this we get $t_{eq} = 2.96 \times 10^4$ which when used in (3.5)-(3.6) we get $(\phi, \dot{\phi}) = (4.42, 5.50 \times 10^{-6})$ which again agrees very well with the numerics. However they don't agree exactly on the time it takes to reach equilibrium point. The numerics say $t_{eq} = 2.61 \times 10^4$ which leads to 13 percent error. These values serve as the initial conditions for the damping phase.

According to the discussion in (3.1.2) we get $a = \sqrt{24\pi V_{eq}} = 3.37865 \times 10^{-5}$ and

$b = V''(\phi_{eq}) = 9.30335 \times 10^{-12}$. Using these we get the damping roots as $\frac{-a \pm \sqrt{a^2-4b}}{2} = (\alpha, \beta) = (-3.35 \times 10^{-5}, -2.78 \times 10^{-7})$. Now we will use (3.15)-(3.16) and the equilibrium values of observables as initial conditions to get the values of $(A, B) = (-0.178, 1.65)$ and thus the damping equations as :

$$\phi = (-0.178)e^{-3.35\times10^{-5}t} + (1.65)e^{-2.78\times10^{-7}t} + 2.95 \tag{4.10}$$

and differentiating this we get $\dot{\phi}$. We can ask when does turnaround happen i.e. when does $\dot{\phi}(t) = 0$? We can solve this using (4.10) for t and then put it back in (4.10) which gives $\phi_{Turn} = 4.55$ whereas numerics give us $\phi_{Turn} = 4.50$ and thus they are in good agreement. Also the above time is not the total time as this t starts from equilibrium point and thus we need to add t_{eq} which gives $t_{Turn} = 1.07 \times 10^5$.

Now for the slow-roll point we ask the following question: since damping starts at what time does the inflaton first satisfy the condition $\left|\frac{\ddot{\phi}}{3H\dot{\phi}}\right| = 0.01$? We can solve this in Mathematica to get t which when used with (4.10) gives us $(\phi, \dot{\phi}) = (4.52, -4.10 \times 10^{-7})$ as opposed to numerics which give $(4.46, -4.04 \times 10^{-7})$ which means they reasonably agree with each other. Actually $\frac{\ddot{\phi}}{3H\dot{\phi}}$ can be ± 0.01. It turns out that for Table 5 both in numerical and analytic cases $\frac{\ddot{\phi}}{3H\dot{\phi}} = 0.01$ marks the beginning of slow-roll whereas for Table 6 it is the other sign. It is remarkable that our analytics don't just predict nearly correct values for the observables but they also mimic the overall physical features. Another physical feature that is mimicked by these analytics is the point where $\ddot{\phi} = 0$. Such a point exists for Table 5 cases but not for Table 6 and the analytics and numerics both agree upon this fact. This is the reason why we chose not to define the beginning of slow-roll as a point where $\ddot{\phi} = 0$ as this is not universal behaviour.

For the slow-roll regime we first ask does the inflaton reach the slow-roll point before reaching the pivot point? If yes then the desired slow-roll compatible with observations (2.10)-(2.15) will happen and then we apply (3.20). For $\phi_B = 2.35$ we get $\phi_{SRA} = 4.52 > \phi_* = 4.406$ thus at the pivot point the inflaton velocity is given by (3.20)

as $\dot{\phi} = -\sqrt{\frac{2\lambda}{3\pi}}\phi_* = -4.04 \times 10^{-7}$. (3.20) can be used to find time t taken from slow-roll point to pivot point which when added to t_{SRA} gives you the total time from bounce till pivot point $t_* = 4.79 \times 10^5$ as opposed to the numerics which give $t_* = 3.58 \times 10^5$. For Table 6 cases, the procedure is very similar except now the inflaton simply starts rolling down the hill from the beginning and thus after the equilibrium point never turns around and hits the slow-roll directly. There too the analytic procedure is similar with some changes in the signs of observables used but at the end the results are in reasonable agreement with numerics.

One important thing to note from Tables 1 and 2 is the difference in predictions for the CRITICAL point i.e the value of ϕ_B after which all intital conditions at the bounce lead to the desired slow-roll. For Table 5 the critical point is 2.23 numerically and 2.30. For Table 6 the critical point is -6.67 numerically and -6.66. This difference comes again because of the approximations used to get analytic solutions which is expected. However the aim of these analytics is not to match each an everything precisely with the numerics, rather what we want is to mimic the general behaviour of primary and secondary observables so that they can be used with confidence in the study of perturbations, in particular derive the interesting results of [19] and [22,23] i.e. power suppression for large angular scales of CMB and the possibility of linking these with non-gaussianity.

In these tables we have not shown any PE dominated cases because there the inflaton hardly from the bounce point to turnaround to the slow-roll point. What we mean is that if we start at $\phi_B = 1600$ then at the turnaround point or the slow-roll point we will have $\phi_{Turn} = \phi_B +$ some small decimal number i.e. the inflaton hardly moves and this agrees with the numerics. This is very similar to the quadratic case.

Event	ϕ_A	$\dot{\phi_A}$	t_A	ϕ_N	$\dot{\phi_N}$	t_N
Bounce	2.20	9.05×10^{-1}	0	2.20	9.05×10^{-1}	0
End of SI	2.34	6.40×10^{-1}	1.80×10^{-1}	2.34	6.40×10^{-1}	1.80×10^{-1}
KE = PE	4.28	5.16×10^{-6}	3.16×10^{4}	4.25	5.09×10^{-6}	2.79×10^{4}
Turn	4.41	0	1.13×10^{5}	4.36	0	1.04×10^{5}
Slow-Roll	4.38	-3.97×10^{-7}	2.00×10^{5}	4.32	-3.91×10^{-7}	2.38×10^{5}
$*$	NA	NA	NA	NA	NA	NA
Bounce	2.23	9.05×10^{-1}	0	2.23	9.05×10^{-1}	0
End of SI	2.37	6.40×10^{-1}	1.80×10^{-1}	2.37	6.40×10^{-1}	1.80×10^{-1}
KE = PE	4.31	5.23×10^{-6}	3.11×10^{4}	4.28	5.15×10^{-6}	2.75×10^{4}
Turn	4.44	0	1.12×10^{5}	4.39	0	1.03×10^{5}
Slow-Roll	4.41	-4.00×10^{-7}	1.98×10^{5}	4.35	-3.94×10^{-7}	2.35×10^{5}
$*$	4.406	-4.04×10^{-7}	2.12×10^{5}	NA	NA	NA
Bounce	2.30	9.05×10^{-1}	0	2.30	9.05×10^{-1}	0
End of SI	2.44	6.40×10^{-1}	1.80×10^{-1}	2.44	6.40×10^{-1}	1.80×10^{-1}
KE = PE	4.37	5.39×10^{-6}	3.02×10^{4}	4.34	5.31×10^{-6}	2.67×10^{4}
Turn	4.50	0	1.09×10^{5}	4.45	0	1.00×10^{5}
Slow-Roll	4.48	-4.06×10^{-7}	1.93×10^{5}	4.41	-4.00×10^{-7}	2.89×10^{5}
$*$	4.406	-4.04×10^{-7}	3.68×10^{5}	4.406	-4.02×10^{-7}	2.47×10^{5}
Bounce	2.35	9.05×10^{-1}	0	2.35	9.05×10^{-1}	0
End of SI	2.49	6.40×10^{-1}	1.80×10^{-1}	2.49	6.40×10^{-1}	1.80×10^{-1}
KE = PE	4.42	5.50×10^{-6}	2.96×10^{4}	4.39	5.43×10^{-6}	2.61×10^{4}
Turn	4.55	0	1.07×10^{5}	4.50	0	9.86×10^{4}
Slow-Roll	4.52	-4.10×10^{-7}	1.89×10^{5}	4.46	-4.04×10^{-7}	2.24×10^{5}
$*$	4.406	-4.04×10^{-7}	4.79×10^{5}	4.406	-4.04×10^{-7}	3.58×10^{5}

Table 5: Comparison of Analytic(A) and Numeric(N) data for the evolution of observables for KE dominated cases with $\phi_B > 0$ for a quartic potential, $V(\phi) = \lambda\phi^4$ where $\lambda = 3.97\times10^{-14}$. Each block represents an initial condition at the bounce and each row within a block represents an event in ascending order: Bounce, End of Superinflation, Equilibrium, Turnaround, Slow-roll and Pivot point. The desired slow-roll happens $\phi_B \geq 2.23$ for analytics and $\phi_B > 2.30$ for numerics.

Event	ϕ_A	$\dot{\phi_A}$	t_A	ϕ_N	$\dot{\phi_N}$	t_N
Bounce	-6.60	9.05×10^{-1}	0	-6.60	9.05×10^{-1}	0
End of SI	-6.46	6.40×10^{-1}	1.80×10^{-1}	-6.46	6.40×10^{-1}	1.80×10^{-1}
KE = PE	-4.54	5.81×10^{-6}	2.80×10^{4}	-4.57	5.88×10^{-6}	2.47×10^{4}
Slow-Roll	-4.33	4.01×10^{-7}	1.40×10^{5}	-4.35	4.02×10^{-7}	2.40×10^{5}
$*$	NA	NA	NA	NA	NA	NA
Bounce	-6.66	9.05×10^{-1}	0	-6.66	9.05×10^{-1}	0
End of SI	-6.52	6.40×10^{-1}	1.80×10^{-1}	-6.52	6.40×10^{-1}	1.80×10^{-1}
KE = PE	-4.60	5.97×10^{-6}	2.73×10^{4}	-4.63	6.05×10^{-6}	2.40×10^{4}
Slow-Roll	-4.40	4.07×10^{-7}	1.37×10^{5}	-4.41	4.08×10^{-7}	2.34×10^{5}
$*$	NA	NA	NA	-4.406	4.06×10^{-7}	2.54×10^{5}
Bounce	-6.67	9.05×10^{-1}	0	-6.67	9.05×10^{-1}	0
End of SI	-6.53	6.40×10^{-1}	1.80×10^{-1}	-6.53	6.40×10^{-1}	1.80×10^{-1}
KE = PE	-4.61	6.00×10^{-6}	2.71×10^{4}	-4.64	6.08×10^{-6}	2.39×10^{4}
Slow-Roll	-4.41	4.08×10^{-7}	1.37×10^{5}	-4.42	4.09×10^{-7}	2.33×10^{5}
$*$	-4.406	4.04×10^{-7}	1.49×10^{5}	-4.406	4.05×10^{-7}	2.80×10^{5}
Bounce	-6.70	9.05×10^{-1}	0	-6.70	9.05×10^{-1}	0
End of SI	-6.56	6.40×10^{-1}	1.80×10^{-1}	-6.56	6.40×10^{-1}	1.80×10^{-1}
KE = PE	-4.65	6.09×10^{-6}	2.68×10^{4}	-4.68	6.17×10^{-6}	2.36×10^{4}
Slow-Roll	-4.44	4.11×10^{-7}	1.35×10^{5}	-4.46	4.12×10^{-7}	2.29×10^{5}
$*$	-4.406	4.04×10^{-7}	2.27×10^{5}	-4.406	4.04×10^{-7}	3.57×10^{6}

Table 6: Comparison of Analytic(A) and Numeric(N) data for the evolution of observables for KE dominated cases with $\phi_B < 0$ for a quartic potential, $V(\phi) = \lambda\phi^4$ where $\lambda = 3.97 \times 10^{-14}$. Each block represents an initial condition at the bounce and each row within a block represents an event in ascending order: Bounce, End of Superinflation, Equilibrium, Turnaround, Slow-roll and Pivot point. The desired slow-roll happens $\phi_B \leq -6.67$ for analytics and $\phi_B \leq -6.66$ for numerics.

5 Conclusion

In this dissertation we showed how one can avoid solving the full non-linear set of equations of LQC and instead divided the full evolution of the scalar field into different regimes and used approximations in each of them to solve the corresponding differential equations easily. Although this introduces errors, we have seen that they are no more than five percent which means our analytic solutions are an excellent approximation to the full numerical solutions. For a number of scalar field potentials, we were able to compare our analytic approximations for each stage of the evolution of the scalar field with the full numerical simulations. The results were very encouraging with differences in the predicted and measured values of the key parameters ϕ and $\dot{\phi}$ being no more than 5 percent. These are all seen in the complete tables for the potentials we have used. In general this method can be applicable to all non-steep potentials even if they have steps, bumps etc. More importantly, with the expressions for observables we have derived in this dissertation, we can use them in the Mukhanov-Sasaki equation i.e. $\chi_k'' + (k^2 - \frac{z''}{z})\chi_k$ where χ_k is the Mukhanov-Sasaki variable, $z = \frac{a\dot{\phi}}{H}$ and $'$ denotes differentiation with respect to conformal time. The $\frac{z''}{z}$ term is a function of the slow-roll parameters and their derivatives i.e. $\epsilon\dot{\epsilon}, \eta, \dot{\eta}$. But each of them can be re-written in terms of the primary observable $\phi, \dot{\phi}$. This will allow us to directly substitute the analytic expressions derived for primary observables in this $\frac{z''}{z}$ term. Then we can either solve the Mukhanov-Sasaki equation numerically or we can try to find patterns and regimes where this equation can be solved analytically. We also discussed how a change in the way we calculate of $\ddot{\phi}$ i.e. instead of $\ddot{\phi} = \frac{d\dot{\phi}}{dt}$ we use $\ddot{\phi} = -3H\dot{\phi} - V'(\phi)$, helps to eradicate any discontinuity in the $\frac{z''}{z}$ term as it then becomes simply a function of the primary observables. Thus the perturbations can now in principle cross-over the equilibrium point safely without creating any unwanted structures in the CMB. So the hope is that by substituting our analytic solutions directly into the Mukhanov-Sasaki equation and then solving it numerically we will have an analytic understanding for arbitrary potentials of the suppression in the power spectrum calculated on large scales which is seen numerically in the context of LQC.

If this happens then we will have an analytic way of understanding how does quantum gravity leads to different results compared to standard inflation. If this is successful, then we can move on to discuss how these analytical techniques help us understand non-Gaussianities in the CMB and thus extract information about the pre-inflationary regime of our primordial universe.

References

[1] K. Becker, M. Becker and J. H. Schwarz, "String theory and M-theory: A modern introduction," Cambridge Univ. Pr. (2007) 739 p

[2] L. McAllister and E. Silverstein, "String Cosmology: A Review," Gen. Rel. Grav. **40**, 565 (2008) [arXiv:0710.2951 [hep-th]].

[3] C. Kiefer, "Quantum gravity," Int. Ser. Monogr. Phys. **124**, 1 (2004) [Int. Ser. Monogr. Phys. **136**, 1 (2007)] [Int. Ser. Monogr. Phys. **155**, 1 (2012)].

[4] R. Gambini and J. Pullin, "A first course in loop quantum gravity," Oxford, UK: Univ. Pr. (2011) 183 p

[5] C. Rovelli, "Quantum gravity," Cambridge, UK: Univ. Pr. (2004) 455 p

[6] C. Rovelli and F. Vidotto, "Covariant Loop Quantum Gravity : An Elementary Introduction to Quantum Gravity and Spinfoam Theory," Cambridge Univ. Pr. (2014) 265 p

[7] J. Ambjorn, J. Jurkiewicz and R. Loll, "Causal Dynamical Triangulations and the Quest for Quantum Gravity," arXiv:1004.0352 [hep-th].

[8] J. Henson, "The Causal set approach to quantum gravity," In *Oriti, D. (ed.): Approaches to quantum gravity* 393-413 [gr-qc/0601121].

[9] A. Ashtekar and P. Singh, "Loop Quantum Cosmology: A Status Report," Class. Quant. Grav. **28**, 213001 (2011) [arXiv:1108.0893 [gr-qc]].

[10] A. Ashtekar, M. Bojowald and J. Lewandowski, "Mathematical structure of loop quantum cosmology," Adv. Theor. Math. Phys. **7**, 233 (2003) [gr-qc/0304074].

[11] A. Ashtekar, T. Pawlowski and P. Singh, "Quantum Nature of the Big Bang: Improved dynamics," Phys. Rev. D **74**, 084003 (2006) [gr-qc/0607039].

[12] A. Ashtekar, T. Pawlowski and P. Singh, "Quantum Nature of the Big Bang: An Analytical and Numerical Investigation. I.," Phys. Rev. D **73**, 124038 (2006) [gr-qc/0604013].

[13] A. Ashtekar, T. Pawlowski and P. Singh, "Quantum nature of the big bang," Phys. Rev. Lett. **96**, 141301 (2006) [gr-qc/0602086].

[14] A. Ashtekar, "Symmetry reduced loop quantum gravity: A birds eye view," Int. J. Mod. Phys. D **25**, no. 08, 1642010 (2016) doi:10.1142/S0218271816420104 [arXiv:1605.02648 [gr-qc]].

[15] E. Alesci and F. Cianfrani, "Quantum-Reduced Loop Gravity: Cosmology," Phys. Rev. D **87**, no. 8, 083521 (2013) [arXiv:1301.2245 [gr-qc]].

[16] J. Lewandowski and H. Sahlmann, Phys. Rev. D **93**, no. 2, 024042 (2016) doi:10.1103/PhysRevD.93.024042 [arXiv:1507.01149 [gr-qc]].

[17] A. Ashtekar, W. Kaminski and J. Lewandowski, "Quantum field theory on a cosmological, quantum space-time," Phys. Rev. D **79**, 064030 (2009) [arXiv:0901.0933 [gr-qc]].

[18] I. Agullo, A. Ashtekar and W. Nelson, "Extension of the quantum theory of cosmological perturbations to the Planck era," Phys. Rev. D **87**, no. 4, 043507 (2013) [arXiv:1211.1354 [gr-qc]].

[19] I. Agullo, A. Ashtekar and W. Nelson, "The pre-inflationary dynamics of loop quantum cosmology: Confronting quantum gravity with observations," Class. Quant. Grav. **30**, 085014 (2013) [arXiv:1302.0254 [gr-qc]].

[20] A. Ashtekar and D. Sloan, "Loop quantum cosmology and slow roll inflation," Phys. Lett. B **694**, 108 (2011) doi:10.1016/j.physletb.2010.09.058 [arXiv:0912.4093 [gr-qc]].

[21] A. Ashtekar and D. Sloan, "Probability of Inflation in Loop Quantum Cosmology," Gen. Rel. Grav. **43**, 3619 (2011) doi:10.1007/s10714-011-1246-y [arXiv:1103.2475 [gr-qc]].

[22] B. Bonga and B. Gupt, arXiv:1510.00680 [gr-qc].

[23] B. Bonga and B. Gupt, Phys. Rev. D **93**, no. 6, 063513 (2016) doi:10.1103/PhysRevD.93.063513 [arXiv:1510.04896 [gr-qc]].

[24] L. Linsefors and A. Barrau, Phys. Rev. D **87**, no. 12, 123509 (2013) doi:10.1103/PhysRevD.87.123509 [arXiv:1301.1264 [gr-qc]].